Communication: Vibrational spectroscopy of atmospherically relevant acid cluster anions: Bisulfate versus nitrate core structures

Tara I. Yacovitch, Nadja Heine, Claudia Brieger, Torsten Wende, Christian Hock, Daniel M. Neumark, and Knut R. Asmis

Citation: The Journal of Chemical Physics **136**, 241102 (2012); doi: 10.1063/1.4732148
View online: http://dx.doi.org/10.1063/1.4732148
View Table of Contents: http://scitation.aip.org/content/aip/journal/jcp/136/24?ver=pdfcov
Published by the AIP Publishing

Communication: Vibrational spectroscopy of atmospherically relevant acid cluster anions: Bisulfate versus nitrate core structures

Tara I. Yacovitch,[1] Nadja Heine,[2] Claudia Brieger,[2] Torsten Wende,[2] Christian Hock,[1] Daniel M. Neumark,[1,3,a)] and Knut R. Asmis[2,b)]
[1]*Department of Chemistry, University of California, Berkeley, California 94720, USA*
[2]*Fritz-Haber-Institut der Max-Planck-Gesellschaft, Faradayweg 4-6, 14195 Berlin, Germany*
[3]*Chemical Sciences Division, Lawrence Berkeley National Laboratory, Berkeley, California 94720, USA*

(Received 25 May 2012; accepted 14 June 2012; published online 28 June 2012)

Infrared multiple photon dissociation spectra for the smallest atmospherically relevant anions of sulfuric and nitric acid allow us to characterize structures and distinguish between clusters with a bisulfate or a nitrate core. We find that bisulfate is the main charge carrier for $HSO_4^- \cdot H_2SO_4 \cdot HNO_3$ but not for $NO_3^- \cdot H_2SO_4 \cdot HNO_3$. For the mixed dimer anion, we find evidence for the presence of two isomers: $HSO_4^- \cdot HNO_3$ and $NO_3^- \cdot H_2SO_4$. Density functional calculations accompany the experimental results and provide support for these observations. © *2012 American Institute of Physics*. [http://dx.doi.org/10.1063/1.4732148]

Negative ionic clusters containing sulfuric acid, nitric acid, and water were first measured in the atmosphere in 1978.[1–3] The smallest mixed composition ions are present in significant proportions in the stratosphere, with $HSO_4^- \cdot HNO_3$ and $HSO_4^- \cdot (HNO_3)_2$ comprising ∼16% and ∼5% of the total observed negative ions at 35 km.[2] Ions in the atmosphere are proposed precursors to binary and ternary aerosol formation.[4] These ternary aerosols themselves play an important role, most notably in the formation of polar stratospheric clouds[5] that catalyze ozone depletion during the polar spring. Despite the extensive mass characterization of the small precursor ions, relatively little is known experimentally about their structure. In particular, the question of charge localization has not been fully addressed. In previous experiments relying on the charge to mass ratio for ion detection,[1–3,6–8] the bisulfate ion (HSO_4^-) was simply assumed to carry the negative charge due to the greater relative gas phase acidity of sulfuric acid versus nitric acid ($\Delta_{acid}G = -1265$ kJ/mol vs -1329.7 kJ/mol).[9] In this paper, we apply infrared multiple photon dissociation (IRMPD) spectroscopy to mass-selected, cryogenically cooled ions in the 550–1850 cm^{-1} spectral range in order to probe the structure of mixed sulfuric and nitric acid deprotonated cluster anions.[10]

Previous IRMPD spectra have been reported for hydrated clusters of nitrate[11] and bisulfate.[12] The bisulfate clusters showed evidence for a continuous elongation of the OH bond with increasing hydration, indicative of the beginnings of water-mediated dissociation, while the nitrate results revealed a high symmetry structure for the $NO_3^- \cdot (H_2O)_3$ cluster, similar to the D_{3h} structure of bare NO_3^-.[13] In both cases, rings of water molecules maximized hydrogen bonding, stabilizing the weakly acidic proton for HSO_4^- and binding to multiple oxygen sites with partial negative charge for both species. Kinetics experiments reacting H_2SO_4 with $NO_3^- \cdot (HNO_3)_n$ showed rapid production of ions with the mass of $HSO_4^- \cdot (HNO_3)_n$ for $n = 1$–3.[7,8]

In this work, IRMPD experiments were carried out on a previously described ring electrode trap/time-of-flight (TOF) mass spectrometer[14,15] using the "Free Electron Laser for Infrared eXperiments" (FELIX).[16] Ions were produced by electrospray of a solution of 25 mM H_2SO_4 and trace amounts of HNO_3 in a 1:4 water:acetonitrile mix. The negative ions were then transferred into a high vacuum system. Parent ions were mass-selected in a quadrupole mass filter and focused into a ring electrode ion trap. To allow for continuous ion loading and ion thermalization, the trap was continuously filled with He gas at an ion-trap temperature of 15 K. After filling the trap for 99 ms, all ions were extracted from the ion trap, focused both temporally and spatially into the center of the extraction region of an orthogonally mounted linear TOF mass spectrometer, and irradiated with a single FELIX macropulse (50 mJ/pulse and ∼0.25% rms bandwidth). Under these conditions, most of the ions are thermalized prior to IR irradiation.[17,18] The IRMPD spectra were recorded by monitoring all ion intensities simultaneously as the laser wavelength is scanned. The photodissociation cross section σ was determined from the relative abundances of the parent and photofragment ions, $I_p(\nu)$ and $I_f(\nu)$, and the frequency-dependent laser power $P(\nu)$ using $\sigma = -\ln[I_p(\nu)/(I_p + I_f)]/P(\nu)$.

The IRMPD spectra for three mixed negatively charged clusters and HSO_4^- are shown as black traces in Fig. 1. These spectra are constructed from multiple data sets over different regions. The strongest peaks appear in the 1100–1500 cm^{-1} region as in the $HSO_4^- \cdot (H_2O)_n$ and $NO_3^- \cdot (H_2O)_n$ spectra,[11–13] and correspond to stretching of the S=O and N=O bonds. Some lower intensity peaks appear at lower frequencies, and an isolated peak appears around 1650 cm^{-1}. Bulk optical constants from the 2002 results of Norman *et al.*[19] for laboratory-generated ternary aerosols (median

a)Electronic mail: dneumark@berkeley.edu.
b)Electronic mail: asmis@fhi-berlin.mpg.de.

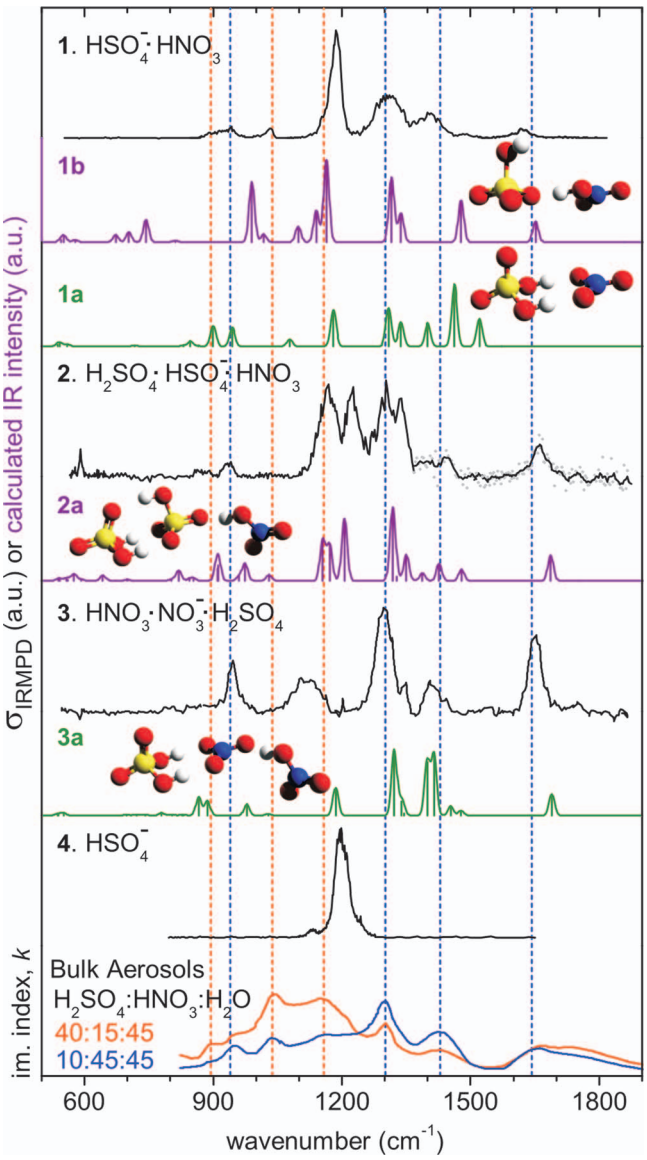

FIG. 1. Experimental spectra (black) for the three mixed clusters and the bare HSO_4^- ion. The 1367–1868 cm^{-1} region of spectrum **2** was smoothed. Best-fit structures for each cluster are shown along with the harmonic frequencies convoluted with a Gaussian of FWHM = 15 cm^{-1} (green for nitrate cores and purple for bisulfate cores). The bottom panel plots bulk spectra from Norman *et al.*[19] and shows the imaginary refractive indices of bulk aerosols with differing weight percent ratios of H_2SO_4:HNO_3:H_2O. Vertical dotted lines line up with bulk peaks attributed by Norman *et al.* to HSO_4^- (orange) and HNO_3 (blue) vibrational modes.

aerosol size <1 μm) are shown in Fig. 1 for comparison. The bulk curves correspond to the imaginary refractive index, *k*. The aerosol data are characterized by their weight ratio of H_2SO_4:HNO_3:H_2O: the orange trace corresponds to a higher sulfuric acid concentration, 40:15:45 wt. %, while the blue trace corresponds to a higher nitric acid concentration, 10:45:45 wt. %. All features in the bulk spectra can be assigned to absorption bands of the individual ionic and molecular constituents (HSO_4^-, HNO_3, and H_2O in this case).[5,19] These contributions are shown as dotted lines in Fig. 1: orange for HSO_4^- and blue for HNO_3.

All three clusters show some resemblance to the bulk aerosol results. Spectra **1** and **2** show a strong peak around 1170 cm^{-1}, matching the prominent HSO_4^- peak at 1195 cm^{-1} in spectrum **4** and the bulk aerosol mode at 1150 cm^{-1}. This feature is missing in spectrum **3**. The most intense peak in spectrum **3** at 1297 cm^{-1} lines up well with a bulk HNO_3 mode. Corresponding features are seen in spectra **1** and **2**, as well. Another key spectral feature is the peak from the combined N=O stretch and NOH bending mode, occuring at 1672 cm^{-1} in the bulk. This peak is well separated from other transitions and is characteristic of intact HNO_3. It appears in bulk solution as well as in all three cluster spectra.

This initial comparison indicates that all three clusters contain HNO_3. In addition, HSO_4^- is present in spectra **1** and **2** but not in **3**, implying that NO_3^- is the charge carrier for this cluster. Spectrum **1** shows a similar pattern of peaks as the bulk results, while spectrum **2** shows all of the aerosol peaks with the addition of two intense transitions at 1224 and 1338 cm^{-1}, an indication that a sum of HSO_4^- and HNO_3 contributions is not sufficient to describe spectrum **2**, and that multi-centered or H_2SO_4 vibrations are necessary.

In order to test these qualititative inferences of cluster structure, electronic structure calculations were performed using the GAUSSIAN 09 program.[20] Initial structures were constructed using a combination of chemical intuition and results from MD conformational searching using Macro-Model 9.9 (Ref. 21) and the OPLS_2005 (Ref. 22) force field. Optimized geometries and harmonic frequencies at the B3LYP/6-311+G(d,p) level of theory were used to determine preliminary energetic ordering and vibrational frequencies, and the lowest energy and best-fit structures were further optimized at the B3LYP/6-311++G(2df,2dp) level. Structures are labeled according to their relative energies, including zero-point energy corrections. Except for **1b**, only the lowest energy structures are shown in Fig. 1 (many more structures are reported in Figs. S1–S4 of the supplementary material[23]). The simulated IR spectra were derived from Gaussian convolutions (FWHM = 15 cm^{-1}) of the stick spectra associated with the harmonic vibrational frequencies and linear absorption intensities. We compare these simulations to our multiple photon experimental results with the caveat that the linear absorption intensities can only approximate the true IRMPD intensities. No frequency scaling factor was used, since the NO and SO vibrations require different corrections to agree with experiment.[24,25]

Several trends are observed in the simulated structures. First, increasing the number of hydrogen bonds to the negative charge center increases the stability of the cluster. Then, for the same number of hydrogen bonds, lower energy structures tend to have a more symmetric solvation of the negative charge with acid molecules on either sides of the charge carrier. This results in "centrally solvated" motifs for the larger clusters **2** and **3**. Finally, families of similar isomers appear at similar energies, showing the same pattern of hydrogen bonds with small differences in geometry such as the orientation of a terminal HNO_3 molecule.

For cluster **1**, the presence of an intact HNO_3 molecule is indicated by the experimental peak at 1621 cm^{-1}. The presence of HSO_4^- is suggested by the peak at 1186 cm^{-1} matching spectrum **4**. **1b** has the appropriate form, $HSO_4^- \cdot HNO_3$. This structure has a single H-bond and a free bisulfate OH.

The three dominant peaks in the 1100–1500 cm^{-1} region are simulated at 1164, 1316, and 1478 cm^{-1}, and are assigned to the three dominant experimental peaks at 1186, 1310, and 1400 cm^{-1} (see Fig. 1). The peak at 1164 cm^{-1} corresponds to a bisulfate S=O stretching and SOH bending mode, analogous to the molecular HNO_3 mode simulated at 1652 cm^{-1}, while the other two peaks are from N=O or combined N=O and S=O stretches. The simulated peaks at 990 cm^{-1} (combined N=O and S=O stretching mode) and at 1098 cm^{-1} (wag of the H-bonded HNO_3 proton) occur between two experimental peaks. These vibrations might correspond to the experimental peaks at 942 and 1031 cm^{-1}, respectively, though this assignment does not conform to the bulk peak assignments and does not account for the experimental peak at 1483 cm^{-1}. An alternate assignment would require the presence of another isomer to account for the low intensity experimental peaks at 890, 1031, and 1483 cm^{-1}. The lowest energy structure for cluster **1** is **1a**, which lies 24.3 kJ/mol below **1b**, and can account for these missing peaks. **1a** has the form $NO_3^- \cdot H_2SO_4$ involving two hydrogen bonds to the nitrate ion. We conclude that both **1a** and **1b** are present in the experimental results. The relative stability of these two structures is of interest, given that the reaction $H_2SO_4 + NO_3^- \rightarrow HSO_4^- + HNO_3$ is exothermic by 63 kJ/mol.[9] However, the addional hydrogen bond in **1a** compared to **1b** (see Fig. 1) compensates for the asymptotic energies, stabilizing **1a** with respect to **1b**.

For cluster **2**, the best fit structure **2a** features an overall $H_2SO_4 \cdot HSO_4^- \cdot HNO_3$ geometry with a centrally solvated charge. While a large number of isomers were found including structures with NO_3^- charge localization and structures with two hydrogen bonds between HSO_4^- and HNO_3, only those structures with the triply hydrogen bound $HSO_4^- \cdot H_2SO_4$ motif present in **2a** had energies below 5 kJ/mol. These four structures, differing only in the placement of the HNO_3, showed reasonable agreement with experiment, though the assignment to **2a** is preferred for energetic reasons.[23] The single $HSO_4^- \cdot HNO_3$ hydrogen bond in **2a** is similar to that found in **1b**, but the OH group on the bisulfate is hydrogen-bonded to the adjacent H_2SO_4.

As mentioned above, the IR spectrum of cluster **3** is quite different from the other two. The best-fit and lowest energy structure **3a** has a negatively charged NO_3^- moiety that is centrally solvated in the cluster. The geometry of **3a** includes the $NO_3^- \cdot H_2SO_4$ dimer motif with two hydrogen bonds, similar to **1a**. The intensities for the peaks at 945 and 1650 cm^{-1} are underestimated in the simulations, but these experimental peaks are also narrower than the others, making them appear stronger. The broadened peak at 1116 cm^{-1} in the experimental results is not well simulated in **3a,** with the closest candidate being the H_2SO_4 combined SO stretch and SOH bending mode at 1185 cm^{-1}. The presence of a small amount of one of the $HSO_4^- \cdot (HNO_3)_2$ isomers **3b** or **3d** (Fig. S3 of the supplementary material) could explain the 1116 cm^{-1} peak. However, these structures also show an intense HNO_3 peak around 1482 cm^{-1}, characteristic of the donor-acceptor HNO_3, which is not apparent in the experiment. For **3**, a large number of low-energy isomers were found, including two interesting families with the same number of hydrogen bonds: $HNO_3 \cdot HSO_4^- \cdot HNO_3$ with a central HSO_4^- charge carrier (>2.7 kJ/mol energy range, includes **3b** and **3d**) and $NO_3^- \cdot H_2SO_4 \cdot HNO_3$ with a terminal NO_3^- charge carrier (>3.4 kJ/mol). The terminal NO_3^- family does not agree with experiment as well as **3a**, while the central HSO_4^- family and the **3a** isomer both show some agreement and some discrepancy with experiment. Ultimately, we prefer to assign the major species in spectrum **3** to the centrally solvated nitrate structure **3a** because of its low energy and complete ion solvation, whereby every NO_3^- oxygen atom receives a hydrogen bond. Cluster **3** highlights the ability of a particularly stable hydrogen-bonded structure to overcome the intrinsic gas phase acidities of the component moieties.

Both of the best fit structures **2a** and **3a** are also the lowest energy isomers. So why does **1b** appear to dominate the spectrum when it is 24 kJ/mol above the global minimum? Previous gas phase IR experiments[26–28] have shown evidence for multiple isomers, and trapping in a local minimum is likely here, too. No other minima are present between 0 and +24 kJ/mol: **1a** is the only stable structure with two hydrogen bonds (all of our calculations of the $HSO_4^- \cdot HNO_3$ structure with two hydrogen bonds and different starting geometries converged to **1a**). While **1b** has greater entropy than **1a**, this cannot account for the full 24 kJ/mol energy difference, even at room temperature.[23] However, formation of $HSO_4^- \cdot HNO_3$ type structures in the precursor droplets is likely since (1) the bulk starting solution contains much HSO_4^- and little NO_3^- by acid-base equilibrium arguments and (2) statistically, many more distinct random starting geometries are possible with a single hydrogen bond than with two. Prior to trapping, we expect some relaxation of the ions but conclude that the barrier to interconversion of **1b** to **1a** is sufficient to trap a portion of the isomers in the **1b** conformer (barrier ~2.7 kJ/mol (Ref. 23)). In addition, it is possible that our experiment is less sensitive to stucture **1a** than **1b**, owing to the requirement that multiple photons be absorbed to observe signal. As this occurs, the cluster heats up. If a vibrational mode of **1a** is being excited, one of the hydrogen bonds will eventually break, at which point isomerization to **1b** will be very facile, since the proton affinity of NO_3^- is greater than that of HSO_4^-. This isomerization can shut off additional photon absorption if the vibrational resonances for vibrationally hot **1b** are different from those for hot **1a**.

An underlying assumption in many published studies on atmospheric ions is that deprotonated clusters of sulfuric and nitric acid behave according to the measured thermodynamics of the individual components.[3,6,7,29] Our results challenge the assumption that the HSO_4^- anion is always the charge carrier in these small mixed clusters by showing compelling evidence that NO_3^- carries the charge in **3**: $H_2SO_4 \cdot NO_3^- \cdot HNO_3$. In the kinetics results of Viggiano *et al.*,[7,8] the existence of clusters of the type $NO_3^- \cdot H_2SO_4$ was not considered based on the thermodynamic arguments above. Our overall findings show that the nitrate ion may indeed be formed within this cluster. These results may motivate further exploration of the structures of these small atmospheric clusters. Clusters **1**, **2**, and **3** are prime targets for OH stretching[30,31] and double-resonance measurements.[32] Such experiments could further

characterize the hydrogen bonding networks and separate isomers such as **1a** and **1b**.

In this paper, we have assigned the charge localization in the deprotonated cluster anions of sulfuric and nitric acid. We find that these small clusters behave quite differently than their individual components in the gas phase or in bulk water, where quantities like gas phase acidity and pH govern interactions. In clusters, these measures of acidity compete with the stabilization energy from multiple H-bonds and from the distribution of negative charge in "centrally solvated" geometries. This is clear for cluster **3** where calculated energetics and spectral assignments show that the negative charge is located on the nitrate moiety rather than the sulfuric acid moiety. Spectrum **2** is assigned to a structure with a solvated HSO_4^- ion, as expected from the bare ion thermodynamics and bulk acid-base considerations. For spectrum **1**, the situation is more complex: the trapped local minimum structure $HSO_4^- \cdot HNO_3$ is observed predominatly together with small amounts of $NO_3^- \cdot H_2SO_4$. These results provide enhanced understanding of the ions present in our atmosphere, and call into question previous assumptions about their structures.

We gratefully acknowledge Jia Zhou, Gabriele Santambrogio, Mathias Brümmer, and Ludger Wöste for their aid in the preliminary measurements on HSO_4^-. We thank the Stichting voor Fundamenteel Onderzoek der Materie (FOM) for granting the required beam time and highly appreciate the skill and assistance of the FELIX staff. This research is funded by the European Community's Seventh Framework Program (FP7/2007-2013, Grant No. 226716) and the (U.S.) Air Force Office of Scientific Research (USAFOSR) (FA9550-09-1-0343). T.I.Y. thanks the National Science and Engineering Research Council of Canada (NSERC) for a postgraduate scholarship. C.H. thanks the German Academic Exchange Service (DAAD) for a postdoctoral scholarship. Calculations were performed at the Molecular Dynamics and Computational Facility at the University of California, Berkeley (National Science Foundation (NSF) Grant No. CHE-0840505).

[1]F. Arnold, H. Bohringer, and G. Henschen, Geophys. Res. Lett. **5**, 653, doi:10.1029/GL005i008p00653 (1978).
[2]E. Arijs, D. Nevejans, P. Frederick, and J. Ingels, Geophys. Res. Lett. **8**, 121, doi:10.1029/GL008i001p00121 (1981).
[3]E. Arijs, Planet Space Sci. **40**, 255 (1992).
[4]A. Sorokin, F. Arnold, and D. Wiedner, Atmos. Environ. **40**, 2030 (2006).
[5]S. E. Anthony, T. B. Onasch, R. T. Tisdale, R. S. Disselkamp, M. A. Tolbert, and J. C. Wilson, J. Geophys. Res. [Atmos.] **102**, 10777, 10.1029/96JD03129 (1997).
[6]A. A. Viggiano, R. A. Perry, D. L. Albritton, E. E. Ferguson, and F. C. Fehsenfeld, J. Geophys. Res., C: Oceans Atmos. **85**, 4551, 10.1029/JC085iC08p04551 (1980).
[7]A. A. Viggiano, M. J. Henchman, F. Dale, C. A. Deakyne, and J. F. Paulson, J. Am. Chem. Soc. **114**, 4299 (1992).
[8]A. A. Viggiano, J. V. Seeley, P. L. Mundis, J. S. Williamson, and R. A. Morris, J. Phys. Chem. A **101**, 8275 (1997).
[9]S. G. Lias and J. E. Bartmess, "Gas phase ion thermochemistry," in *NIST Chemistry WebBook, NIST Standard Reference Database Number 69*, edited by P. J. Linstrom and W. G. Mallard (National Institute of Science and Technology, Gaithersburg, MD), see http://webbook.nist.gov.
[10]K. R. Asmis and D. M. Neumark, Acc. Chem. Res. **45**, 43 (2012).
[11]D. J. Goebbert, E. Garand, T. Wende, R. Bergmann, G. Meijer, K. R. Asmis, and D. M. Neumark, J. Phys. Chem. A **113**, 7584 (2009).
[12]T. I. Yacovitch, T. Wende, L. Jiang, N. Heine, G. Meijer, D. M. Neumark, and K. R. Asmis, J. Phys. Chem. Lett. **2**, 2135 (2011).
[13]R. A. Relph, J. C. Bopp, M. A. Johnson, and A. A. Viggiano, J. Chem. Phys. **129**, 064305 (2008).
[14]D. J. Goebbert, G. Meijer, and K. R. Asmis, AIP Conf. Proc. **1104**, 22 (2009).
[15]D. J. Goebbert, T. Wende, R. Bergmann, G. Meijer, and K. R. Asmis, J. Phys. Chem. A **113**, 5874 (2009).
[16]D. Oepts, A. F. G. van der Meer, and P. W. van Amersfoort, Infrared Phys. Technol. **36**, 297 (1995).
[17]T. Wende, J. Dobler, L. Jiang, P. Claes, E. Janssens, P. Lievens, G. Meijer, K. R. Asmis, and J. Sauer, Int. J. Mass Spectrom. **297**, 102 (2010).
[18]L. Jiang, T. Wende, R. Bergmann, G. Meijer, and K. R. Asmis, J. Am. Chem. Soc. **132**, 7398 (2010).
[19]M. L. Norman, R. E. Miller, and D. R. Worsnop, J. Phys. Chem. A **106**, 6075 (2002).
[20]M. J. Frisch, G. W. Trucks, H. B. Schlegel *et al.*, GAUSSIAN 09, Revision C.01, Gaussian, Inc., Wallingford, CT, 2010.
[21]MacroModel (Schrödinger, LLC, New York, 2011).
[22]J. L. Banks, H. S. Beard, Y. X. Cao, A. E. Cho, W. Damm, R. Farid, A. K. Felts, T. A. Halgren, D. T. Mainz, J. R. Maple, R. Murphy, D. M. Philipp, M. P. Repasky, L. Y. Zhang, B. J. Berne, R. A. Friesner, E. Gallicchio, and R. M. Levy, J. Comput. Chem. **26**, 1752 (2005).
[23]See supplementary material at http://dx.doi.org/10.1063/1.4732148 for full GAUSSIAN 09 citation, simulated spectra, peak positions and assignments, thermodynamic calculations, potential energy surface scans, and Gaussian output files containing 3D structures and normal mode coordinates for **1a**, **1b**, **2a**, and **3a**.
[24]J. M. Standard, I. S. Buckner, and D. H. Pulsifer, J. Mol. Struct.: THEOCHEM **673**, 1 (2004).
[25]Y. Bouteiller, Chem. Phys. **314**, 159 (2005).
[26]J. P. Beck and J. M. Lisy, J. Phys. Chem. A **114**, 10011 (2010).
[27]J. R. Roscioli and M. A. Johnson, J. Chem. Phys. **126**, 024307 (2007).
[28]G. Gregoire, N. R. Brinkmann, D. van Heijnsbergen, H. F. Schaefer, and M. A. Duncan, J. Phys. Chem. A **107**, 218 (2003).
[29]F. Arnold and G. Henschen, Nature (London) **275**, 521 (1978).
[30]J. P. Beck and J. M. Lisy, J. Chem. Phys. **135**, 044302 (2011).
[31]B. Bandyopadhyay and M. A. Duncan, Chem. Phys. Lett. **530**, 10 (2012).
[32]C. M. Leavitt, A. B. Wolk, J. A. Fournier, M. Z. Kamrath, E. Garand, M. J. Van Stipdonk, and M. A. Johnson, J. Phys. Chem. Lett. **3**, 1099 (2012).